Molecular Biology of the Cell
Vol. 17, 3435–3445, August 2006

Lymphocyte Chemotaxis Is Regulated by Histone Deacetylase 6, Independently of Its Deacetylase Activity[V]

J. Román Cabrero,*† Juan M. Serrador,*†‡ Olga Barreiro,* María Mittelbrunn,* Salvador Naranjo-Suárez,* Noa Martín-Cófreces,* Miguel Vicente-Manzanares,* Ralph Mazitschek,§ James E. Bradner,§ Jesús Ávila,‖ Agustín Valenzuela-Fernández,* and Francisco Sánchez-Madrid*

*Servicio de Inmunología, Hospital de la Princesa, Universidad Autónoma de Madrid, 28006 Madrid, Spain; ‡Centro Nacional de Investigaciones Cardiovasculares (CNIC), Unidad Mixta CNIC-Universitat de Valencia, 46010 Valencia, Spain; §Chemical Biology Program, The Broad Institute of Harvard University and Massachusetts Institute of Technology, Cambridge, MA 02141; and ‖Centro de Biología Molecular Severo Ochoa, Consejo Superior de Investigaciones Cientificas, Universidad Autónoma de Madrid, Cantoblanco, 28049 Madrid, Spain

Submitted January 4, 2006; Revised May 17, 2006; Accepted May 18, 2006
Monitoring Editor: Martin A. Schwartz

In this work, the role of HDAC6, a type II histone deacetylase with tubulin deacetylase activity, in lymphocyte polarity, motility, and transmigration was explored. HDAC6 was localized at dynamic subcellular structures as leading lamellipodia and the uropod in migrating T-cells. However, HDAC6 activity did not appear to be involved in the polarity of migrating lymphocytes. Overexpression of HDAC6 in freshly isolated lymphocytes and T-cell lines increased the lymphocyte migration mediated by chemokines and their transendothelial migration under shear flow. Accordingly, the knockdown of HDAC6 expression in T-cells diminished their chemotactic capability. Additional experiments with HDAC6 inhibitors (trichostatin, tubacin), other structural related molecules (niltubacin, MAZ-1391), and HDAC6 dead mutants showed that the deacetylase activity of HDAC6 was not involved in the modulatory effect of this molecule on cell migration. Our results indicate that HDAC6 has an important role in the chemotaxis of T-lymphocytes, which is independent of its tubulin deacetylase activity.

INTRODUCTION

Lymphocyte migration is essential for the activity of the immune system in physiological conditions and during adaptive immune responses. Lymphocyte chemotaxis requires the coordinated activity of adhesion and chemotactic receptors, signaling molecules, and cytoskeleton (Vicente-Manzanares and Sanchez-Madrid, 2004). Chemokines are a family of low-molecular-weight cytokines that bind to G protein–coupled receptors on the cell surface (Mackay, 2001). In addition to their classical function as chemoattractants, chemokines modulate lymphocyte adhesion to endothelium, through a yet-poorly understood mechanism of receptor cross-talk between chemotactic and adhesion receptors (Alon and Feigelson, 2002; von Andrian and Mackay, 2000). Chemokines also trigger the remodeling of cytoskeleton and the reorganization of multiple plasma membrane receptors and signaling molecules, which result in an overall change of lymphocyte shape and the acquisition of a migratory, polarized morphology (Sanchez-Madrid and del Pozo, 1999). Lymphocyte polarization involves the generation of two well-differentiated poles. The leading edge clusters actin microfilaments, actin-associated proteins, and signaling molecules that generate protrusive structures, and concentrates adhesion receptors at the cell front. On the other hand, adhesions are released at the rear trailing edge to enable net cell movement (Serrador *et al.,* 1999; Worthylake and Burridge, 2001; Etienne-Manneville and Hall, 2002; Ridley *et al.,* 2003; Vicente-Manzanares and Sanchez-Madrid, 2004).

Although there is much knowledge on how the actin cytoskeleton participates in cell migration (Pantaloni *et al.,* 2001; Pollard and Borisy, 2003), the role played by tubulin and associated proteins in this process remains controversial and seems cell type-dependent (Wittmann and Waterman-Storer, 2001; Destaing *et al.,* 2005). However, it is clear that, in addition to their role during cell division, microtubules play important functions in the establishment and maintenance of cell polarity and adhesion (Prescott *et al.,* 1989; Tannenbaum and Slepecky, 1997; Moreno and Schatten, 2000; Small and Kaverina, 2003). The majority of interphase microtubules are dynamic, but a small proportion is relatively stable (Schulze and Kirschner, 1987), showing a low rate of depolymerization by colchicine or cold. Microtubule

This article was published online ahead of print in *MBC in Press* (http://www.molbiolcell.org/cgi/doi/10.1091/mbc.E06–01–0008) on May 31, 2006.

[V] The online version of this article contains supplemental material at *MBC Online* (http://www.molbiolcell.org).

† These authors contributed equally to this work.

Address correspondence to: F. Sánchez-Madrid (fsanchez.hlpr@salud.madrid.org).

Abbreviations used: TSA, trichostatin A; NCD, nocodazole; TXL, Taxol; PBL, peripheral blood lymphocyte; FN, fibronectin; MTOC, microtubule-organizing center; Tbc, tubacin; HUVEC, human umbilical vein endothelial cells.

stability is related to post-translational modifications of tubulin subunits (Gundersen *et al.*, 1998), including the acetylation of the Lys40 ε-amino group of α-tubulin (L'Hernault and Rosenbaum, 1983; Piperno and Fuller, 1985). This type of acetylation has been found in a variety of proteins (transcription and nuclear import factors, histones) and is catalyzed by a wide range of acetyltransferases (Kouzarides, 2000; Polevoda and Sherman, 2002). In cultured cells, acetylation seems to preferentially occur in polymerized microtubules (Piperno *et al.*, 1987). It has been shown that in vivo, deacetylation takes place on tubulin dimers, rather than microtubules (Matsuyama *et al.*, 2002).

HDAC6, a class II histone deacetylase mainly localized in the cytoplasm (Verdel *et al.*, 2000; Bertos *et al.*, 2004), has two catalytic domains with deacetylase activity. The C-terminal domain is able to deacetylate α-tubulin both in vitro and in vivo, and this activity is reversibly inhibited by trichostatin A (TSA) and tubacin. TSA is a broad HDACs inhibitor, whereas tubacin is specific for the tubulin deacetylase activity of HDAC6 (Hubbert *et al.*, 2002; Matsuyama *et al.*, 2002; Haggarty *et al.*, 2003; Zhang *et al.*, 2003). These compounds inhibit the HDAC6 deacetylase activity by chelating a Zn^{2+} cation (Furumai *et al.*, 2001; Jose *et al.*, 2004) and may also alter the formation of dynamic molecular complexes of HDAC6 with other intracellular proteins such PP1, HSP90, Dia2, dynein, or tubulin (Kawaguchi *et al.*, 2003; Brush *et al.*, 2004; Destaing *et al.*, 2005; Hideshima *et al.*, 2005; Kovacs *et al.*, 2005). In this regard, it has been reported that TSA disrupts HDAC6/PP1 association, affecting the enzymatic activity of both molecules (Brush *et al.*, 2004).

We have herein investigated the role of HDAC6 in the migration of T-lymphocytes. We found that HDAC6 is mainly concentrated at cellular regions with high protrusive activity in migrating lymphocytes and that its expression modulates lymphocyte chemotaxis independently of its enzymatic activity.

MATERIALS AND METHODS

Reagents and Antibodies

Trichostatin A (TSA), nocodazole (NCD), and paclitaxel (Taxol; TXL) were purchased from Calbiochem (San Diego, CA). SDF-1α was from R&D Systems (Minneapolis, MN), and sodium butyrate from Sigma Chemical Co. (St. Louis, MO). Tubacin, DHM-tubacin, niltubacin, MAZ-1391, MAZ-1338, and MAZ-1380 were synthesized according to Mazitschek *et al.* (unpublished data). The 80-kDa fibronectin fragment (FN80) was a generous gift from Dr. A. García-Pardo (Centro de Investigaciones Biológicas, Madrid, Spain). Phytohemaglutinin A (PHA) and interleukin-2 (IL-2) were from Sigma. Rabbit and goat anti-human HDAC6 polyclonal antibodies were purchased from MBL (Watertown, MA) and Santa Cruz Biotechnology (Santa Cruz, CA), respectively. The anti-α-tubulin B-5–1-2 monoclonal antibody (mAb), the FITC-conjugated anti-α-tubulin (clone DM1A), and the anti-acetylated α-tubulin 6–11B-1 mAbs were purchased from Sigma. The JL-8 anti-GFP mAb was from BD Biosciences Clontech (Palo Alto, CA). For surface molecule staining, the following mAbs were used: HP2/19 anti-ICAM-3, 12G5 anti CXCR4, MAB181 anti-CCR5, PL-1 anti-PSGL-1, anti-CD62L, Lia3/2 anti-CD18, HP2/21 anti-CD43 and HUTS-21 anti-activated β1 integrins.

Cells

Human T-cell lines HSB-2 and CEM 1.3 were grown in RPMI 1640 culture medium (Invitrogen, Gaithersburg, MD) supplemented with 10% fetal calf serum (FCS). Human peripheral blood lymphocytes (PBLs) were obtained as described by Campanero *et al.* (1994), and T lymphoblasts by 48-h treatment with 1 μg/ml PHA, followed by 50 U/ml IL-2 in RPMI 1640 medium until the eleventh day.

Transfection of Cells and Recombinant DNA Constructs

PBLs were washed once in phosphate-buffered saline and resuspended (1.2×10^7 cells/ml) in electroporation buffer containing 12 μg of plasmid DNA pEGFP, wtHDAC6-EGFP or double mutant HDAC6 H216A/H611A-EGFP (HDAC6 DD). Cell suspensions (100 μL) were transferred to a 2.0-mm elec-

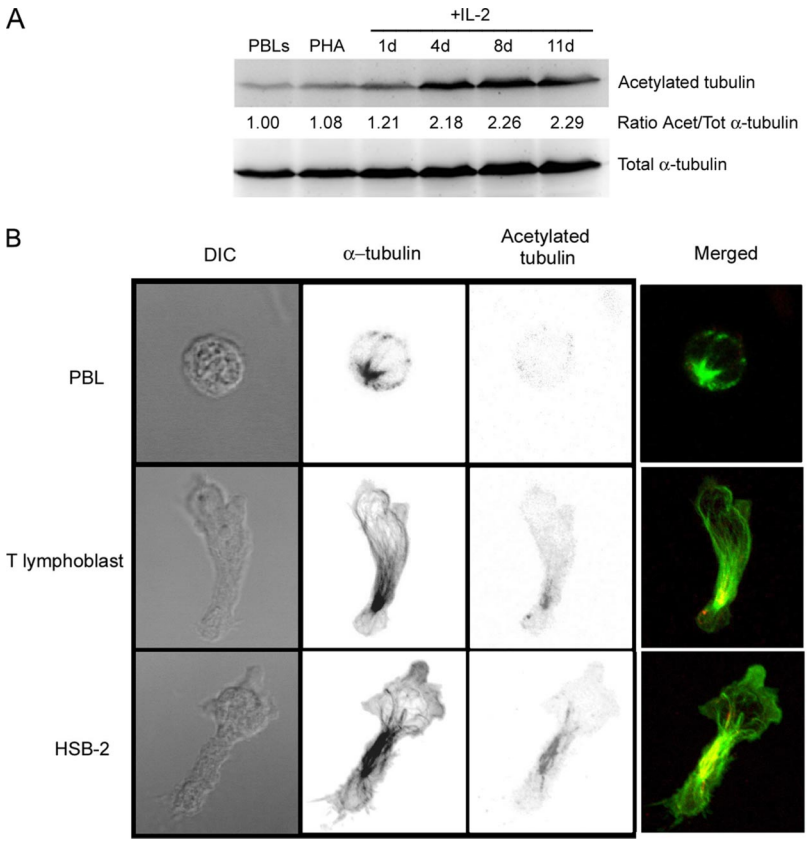

Figure 1. Tubulin acetylation increases during T-lymphocyte activation. (A) PBLs were incubated with PHA (1 μg/ml) for 48 h, washed, and cultured in the presence of 50 U/ml IL-2. At indicated times, cells were sonicated and cell lysates were subjected to SDS-PAGE and immunoblot for detecting total and acetylated tubulin, as stated in *Materials and Methods*. The progressive increase in acetylated tubulin during lymphocyte activation, and the values of the acetylated/total tubulin ratio are shown. (B) Double immunofluorescence staining for tubulin (green fluorescence) and acetylated tubulin (red fluorescence) in resting PBLs, T-lymphoblasts, and HSB-2 T-cells. The predominant localization of acetylated tubulin in bundles around MTOC is shown.

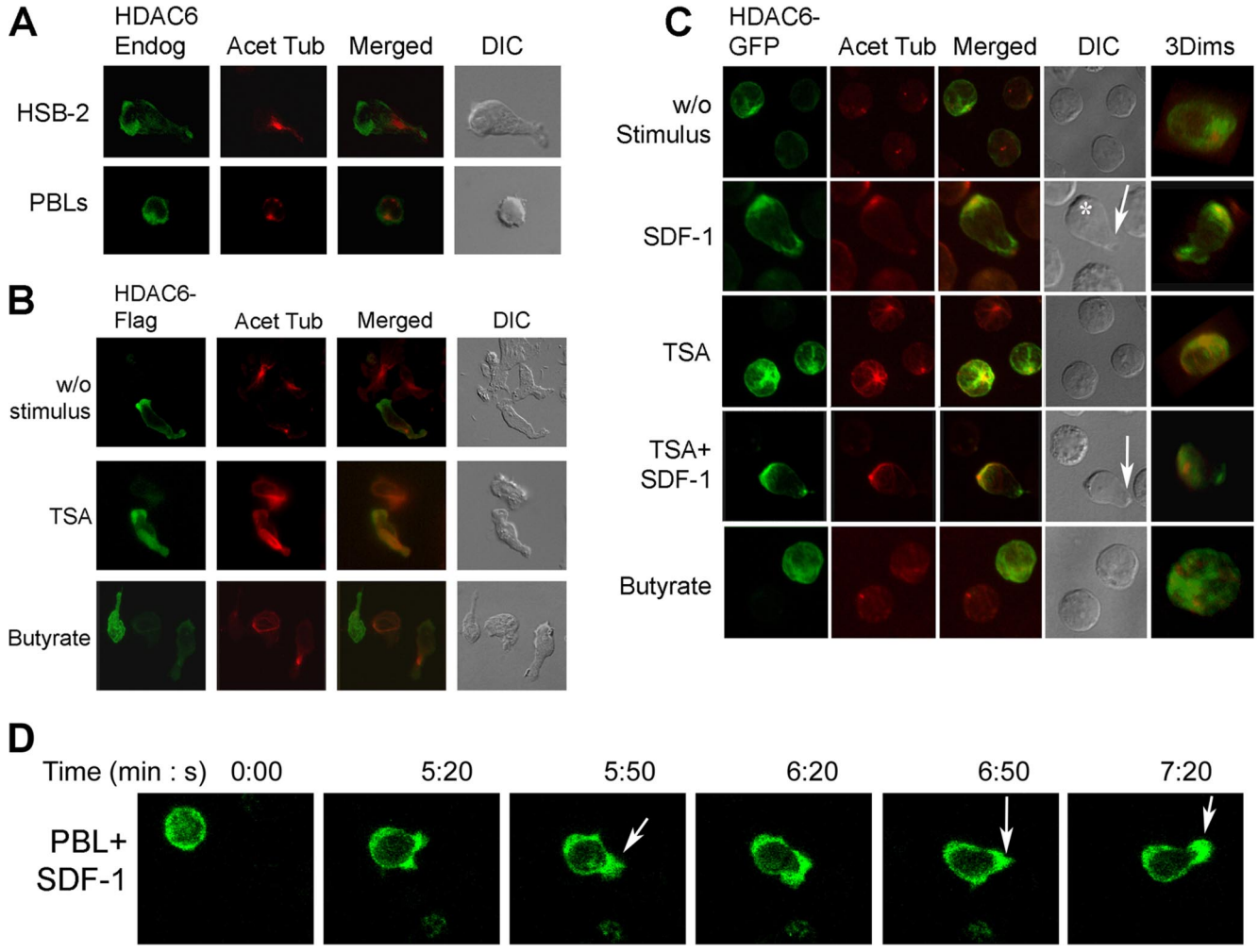

Figure 2. HDAC 6 and acetylated tubulin localization in motile T-lymphocytes. (A) Localization of endogenous HDAC6 and acetylated tubulin in HSB-2 cells and PBLs. Cells adhered to FN-coated coverslips were fixed, permeabilized, and double-stained for HDAC6 and acetylated tubulin. (B) HDAC6-Flag–transfected HSB-2 cells pretreated with the indicated drugs were adhered to FN-coated coverslips and stained with antibody against acetylated tubulin and HDAC6-Flag, as stated in *Materials and Methods.* (C) HDAC6-GFP–transfected PBLs incubated with the indicated stimuli and adhered to 50 μg/ml FN were fixed, permeabilized, and stained for acetylated tubulin. Arrows pointed to leading edge and the asterisk stands on the rear pole in the SDF-1α–polarized PBLs. (D) Time-lapse sequence of HDAC6-GFP–expressing PBLs transfected by nucleofection. Cells were allowed to adhere to FN and stimulated with 100 ng/ml SDF-1α at time zero. Then, cells were analyzed for 7 min by time-lapse confocal microscopy, as stated in *Materials and Methods.* Arrows pointed to the leading edge in the SDF-1α–polarized migrating PBLs.

troporation cuvette and nucleofected with an Amaxa Nucleofector apparatus (Amaxa GmbH, Cologne, Germany). Then, cells were transferred to complete medium without antibiotic and cultured in six-well plates at 37°C until analysis. HSB-2 cells were transfected by electroporation. The human T-cell line CEM 1.3 was transduced with the retroviral vector pLZR IRES to stably express EGFP, wtHDAC6-EGFP, or HDAC6 H216A/H611A-EGFP. Retroviruses were produced by transfection of the Phoenix packaging cell line with a DNA mixture containing 2.5 μg *env* (pVSV-G; Clontech, BD Biosciences), 4 μg *gag-pol* (pNGVL3-MLV) and 3.5 μg retroviral vector pLZR IRES (a generous gift from Dr. A. Bernad, Centro Nacional de Biotecnología, Cantoblanco, Madrid, Spain). Supernatant with retroviruses was recovered and filtered 48 h after transfection and diluted 1:2 in RPMI 1640 medium. The infection was carried out by spinning 5.0×10^5 CEM cells, with 200 μl of retroviral supernatant and polybrene at 6 μg/ml, per well (24-well plates, Costar, Corning, NY), at 1800 rpm, 30°C for 90 min. Finally, 300 μl of complete RPMI medium was added, and cells were cultured at 37°C in 5% CO_2 atmosphere.

siRNA Assay

Double-stranded siRNA (21 pb) against the HDAC6 217–237 (Hubbert *et al.*, 2002; Serrador *et al.*, 2004) and 284–304 sequences, and the negative control was purchased from Eurogentec (Hampshire, United Kingdom). PBL cells (7.0×10^6) were nucleofected with the siRNA using the Human T-Cell nucleofector kit (Amaxa GmbH). Efficiency was assessed by Western blot.

Immunofluorescence Microscopy

These assays were performed as described (Serrador *et al.*, 2004). Briefly, 5.0×10^5 cells were allowed to adhere to coverslips coated with FN80. When indicated, cells were pretreated or not with SDF-1α, TSA, TSA+SDF-1α, NCD, TXL, or sodium butyrate. Cells were then fixed and stained for acetylated and total α-tubulin using the 6-11B-1 and DM1A antibodies. Endogenous HDAC6 was stained with the goat anti-HDAC6 antibody and a secondary donkey anti-goat Alexa-488–conjugated antibody. Cells were observed in a Leica DMR photomicroscope (Leica, Mannheim, Germany), and images were visualized, processed, and stored by using the Leica QFISH software.

Time-Lapse Fluorescence Confocal Microscopy

PBL or CEM cells (5×10^5) were allowed to adhere on FN-coated coverslips, maintained in 1 ml of 2% BSA Hanks' balanced salt solution (HBSS) on Attofluor open chambers (Molecular Probes, Eugene, OR), and placed on the microscope stage. Cells were maintained at 37°C in a 5% CO_2 atmosphere. Series of fluorescence and differential interference contrast frames were ob-

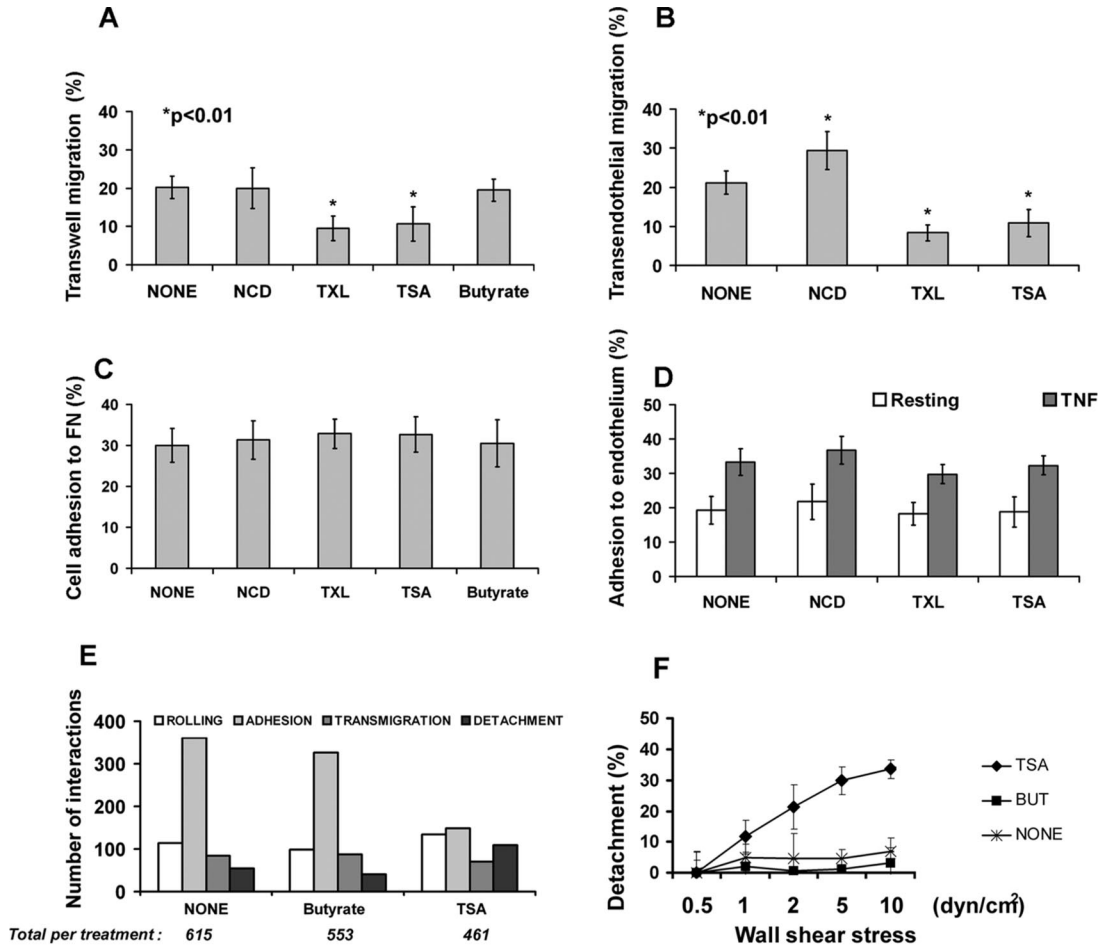

Figure 3. Effect of HDAC6 inhibitor TSA on PBL chemotaxis and adhesion. PBLs were incubated with the indicated drugs (1 mM butyrate, 10 nM TXL, 5 μg/ml NCD, or 5 μM TSA) and the following assays performed: (A) Chemotaxis assays in Transwell chambers. PBLs were allowed to migrate toward 100 ng/ml SDF-1α. The percentage of migrated cells $\pm$ SD is shown. (B) Transmigration across TNF-α–activated endothelium in Transwell chambers. The percentage of migrated cells $\pm$ SD is shown. (C) Adhesion to fibronectin. The percentage of adhered cells $\pm$ SD is shown. (D) Adhesion to resting (white bars) or TNF-α activated (dark gray bars) endothelium. The percentage of adhered cells $\pm$ SD is shown. (E) Lymphocyte transendothelial migration under physiological shear flow conditions across TNF-α–activated HUVEC cells. The number of rolling (white bars), adhered (light tone gray bars), transmigrating (dark gray bars), and detached (black bars) cells $\pm$ SD is shown and was calculated as described in *Material and Methods.* (F) TSA treatment augments PBL detachment under shear stress. The percentage of detached cells was analyzed in seven different fields under increasing flow rates, ranging from 0.5 to 10 dyn/cm^2 of wall shear stress, and is represented as the mean $\pm$ SD. ($\times$), control PBLs without treatment; ■, 1 mM sodium butyrate; ◆, 5 μM TSA pretreatment, 1 h.

tained simultaneously, using a Leica TCS SP confocal laser scanning unit attached to a Leica DMIRBE inverted epifluorescence microscope.

Chemotaxis Assay in Transwell Chambers

Assays for lymphocyte chemotaxis were performed in nude or TNF-α–activated human umbilical vein endothelial cells (HUVEC)-coated polycarbonate membranes of 6.5-mm diameter, 10-μm thickness, and 3- or 5-μm-diameter pore size Transwell chambers (Costar). Lymphocytes (100 μl at 1.0 $\times$ 10^6 cells/ml) resuspended in 0.5% human serum albumin RPMI 1640 were added to the upper chamber. Then, chemokines (100 ng/ml SDF-1α) were added to the lower chamber, and cells were allowed to migrate for 2 h at 37°C in 5% CO_2 atmosphere. Then, the migrated cells were recovered and counted by flow cytometry.

Transendothelial Migration under Flow Conditions

The parallel plate flow chamber used for leukocyte adhesion and transmigration under defined laminar flow has been described (Barreiro *et al.*, 2002). PBL or CEM T-cells (10^6/ml) were drawn on a TNF-α–activated confluent endothelial monolayer at an estimated wall shear stress of 1.8 dyn/cm^2 for a total perfusion time of 10 min. Lymphocyte rolling on the endothelium was easily visualized because they traveled more slowly than free-flowing cells. Lymphocytes were considered to be adherent after 20 s of stable contact with the cell monolayer. Transmigrated lymphocytes were determined as being beneath the endothelial monolayer. Lymphocytes were considered detached when they returned to free-flowing after their complete arrest on endothelium. The number of rolling, adhered, transmigrated, and detached cells was quantified by direct visualization of eight different fields (20$\times$ phase-contrast objective) at each time point of every independent experiment.

For detachment experiments, PBLs untreated or pretreated with TSA or sodium butyrate for 1 h were allowed to adhere for 4 min at 37°C to activated HUVEC monolayers. Then, shear stress was applied by pulling assay buffer (HBSS buffer with 2% FCS) through the flow chamber with a calibrated programmable pump, starting at 0.5 dyn/cm^2 and increasing up to 10 dyn/cm^2 at 1-min intervals. Attached and transmigrated cells after each shear stress interval were quantified (20$\times$ phase-contrast objective), and the mean $\pm$ SD of seven fields is presented. Cell detachment was obtained from the difference of final to initial adhered plus transmigrated cells (Barreiro *et al.*, 2005).

Western Blot Analysis

Cell lysates were subjected to 10% SDS-PAGE under reducing conditions, and transferred onto nitrocellulose membranes (Trans-Blot, Bio-Rad, Hercules, CA). Then, membranes were saturated with tris-buffered saline-0.1% Tween containing 3% BSA and incubated with mAb against α-tubulin or acetylated-

Table 1. Effect of TSA, tubacin, and niltubacin on lymphocyte adhesion and chemokine receptor expression

A

Molecule	Control	TSA (5 μM)
CXCR4	640.41	631.03
CCR5	38.31	43.11
PSGL-1	313.93	321.39
CD62L	558.26	540.46
CD18	423.79	472.97
ICAM3	719.08	752.29
Activated β1 integrins	59.33	50.37
CD43	751.51	841.03

B

Molecule	Control	Tubacin (25 μM)	Niltubacin (25 μM)
CXCR4	45.95	43.37	45.51
CCR5	4.17	4.81	3.78
PSGL1	18.25	18.51	12.75
CD18	12.33	10.27	11.01
ICAM3	31.89	30.79	26.77
Activated β1 integrins	5.46	5.68	4.58
CD43	96.01	130.48	87.95

(A) PBLs were treated or not with TSA for 1 h and analyzed by flow cytometry (arbitrary units). (B) CEM cells were treated as indicated over 6 h and then analyzed by flow cytometry (arbitrary units, Geo Mean).

α-tubulin or HDAC6 or GFP, followed by a peroxidase-conjugated secondary antibody. Proteins were visualized by enhanced chemiluminescence, and densitometric analyses were performed with ImageGauge 3.46 software (Fuji Photo Film Co., Tokyo, Japan).

Tubacin-niltubacin competition assays were carried out for 120 min at 37°C and 5% CO_2 in CEM leukemic T-cells and PBLs. Tubacin (0.25 or 0.5 μM) was coincubated with at least eight different concentrations, from 1 nM to10 μM, of niltubacin to determine IC_{50} (concentration [M] of this competing ligand that inhibits by 50% the effect of tubacin binding). Western blotting of acetylated tubulin resulting from the competitive effect of niltubacin versus tubacin for HDAC6 was then performed. Data were analyzed using GraphPad Prism 2.0 software (GraphPad Software, San Diego, CA).

RESULTS

HDAC6 Is Concentrated in Motile Structures of Polarized Migrating Lymphocytes

To explore the role of HDAC6 in lymphocyte polarity, we first determined the possible relationship between the levels of acetylated tubulin and the polarized shape of T-cells. As expected, we found an increase in total tubulin in PBLs activated with PHA and cultured with IL-2 that peaked between days 4 and 8 (Figure 1A, bottom panel). However, the increase in the levels of acetylated tubulin reached maximal levels at day 8 of cell culture (Figure 1A, top, and B). Acetylated microtubules were preferentially organized in bundles around the microtubule-organizing center (MTOC) within the cellular uropod (Figure 1B). Likewise, HSB-2 T-cells, which exhibit a constitutively polarized morphology (Serrador *et al.*, 1997), also displayed significant amounts of acetylated α-tubulin concentrated at their uropods (Figure 1B).

We then assessed the subcellular localization of HDAC6 in polarized migrating lymphocytes. Immunofluorescence experiments showed that HDAC6 was mainly concentrated at the front lamellipodium of polarized cells and evenly distributed in resting PBLs (Figure 2A). On the other hand, in HSB-2 cells or PBLs transfected with either flag- or GFP-tagged HDAC6, this enzyme was concentrated at the uropod and the leading edge (Figure 2, B–D). This localization was maintained when cells were treated with TSA or sodium butyrate, a HDACs inhibitor that lacks activity on HDAC6 (Serrador *et al.*, 2004).

The effect of HDAC6 overexpression on microtubule acetylation was also studied. Tubulin acetylation levels were reduced in cells overexpressing HDAC6 (Figure 2, B and C), an effect that was inhibited by TSA (Figure 2, B and C). In TSA-treated cells, HDAC6 colocalized with acetylated microtubules (Figure 2, B and C). Chemokines have been reported as main inducers of lymphocyte polarity (del Pozo *et al.*, 1995). When TSA-treated PBLs were induced to polarize with SDF-1α, they acquired a polarized migratory morphology, and HDAC6 was redistributed to the leading edge and the uropod (Figure 2, C and D). Live-cell time-lapse confocal videomicroscopy confirmed the localization of HDAC6 at motility-associated structures in PBLs transfected with HDAC6-GFP and stimulated with SDF-1α (Figure 2D and sal material, Supplementary Video 1).

Lymphocyte Transmigration Inhibition by HDAC6 Inhibitor TSA

We then investigated the role of HDAC6 in lymphocyte migration. Pretreatment of PBLs with TSA for 1 h (to avoid its effect on gene transcription) decreased lymphocyte chemotaxis and their transendothelial migration (Figure 3A, and B). Similar results were observed in HSB-2 and CEM T-cells (unpublished data). The inhibitory effect of TSA was more evident when lymphocytes were allowed to transmigrate across the endothelial cell monolayer. On the other hand, treatment of lymphocytes with TXL decreased cell migration, whereas NCD had an opposing effect (Figure 3B). Additional experiments showed that TSA did not have a significant effect on T-cell adhesion or the expression of chemokine and adhesion receptors (Figure 3, C and D, and Table 1A).

The role of HDAC6 activity in T-cell migration was also analyzed under flow conditions. Although butyrate did not significantly affect any step of lymphocyte transendothelial migration, TSA-treated cells showed a reduced adhesion to the activated endothelium under shear stress, and the detachment rate was significantly higher compared with untreated or butyrate-treated cells (Figure 3E). Furthermore, cell detachment assays at increasing shear flow showed that the binding strength of either untreated or butyrate-treated PBLs adhered to activated endothelial cells was higher than that of TSA-treated PBLs (Figure 3F). These findings indicate that TSA negatively affects lymphocyte extravasation, mainly their firm adhesion to endothelium under flow stress conditions, an effect that is not evident under static conditions. This could be due to blockage of deacetylase activity and/or disruption of HDAC6 molecular complexes by TSA (Brush *et al.*, 2004).

Deacetylase Activity of HDAC6 Is Not Involved in Lymphocyte Migration

To further explore the role of HDAC6 enzymatic activity in lymphocyte migration, we used tubacin (a specific HDAC6 tubulin deacetylase inhibitor), and other deacetylase inactive tubacin derivatives (niltubacin, MAZ-1391, MAZ-1338, and MAZ-TBDPS-O-1380) (Figure 4, A and B). Tubacin inhibits HDAC6 tubulin deacetylase activity in a dose-dependent manner, reaching a plateau at 10–20 μM, whereas niltubacin did not exert any effect at the same doses (Figure 4B and unpublished data). Tubacin inhibited the chemotaxis

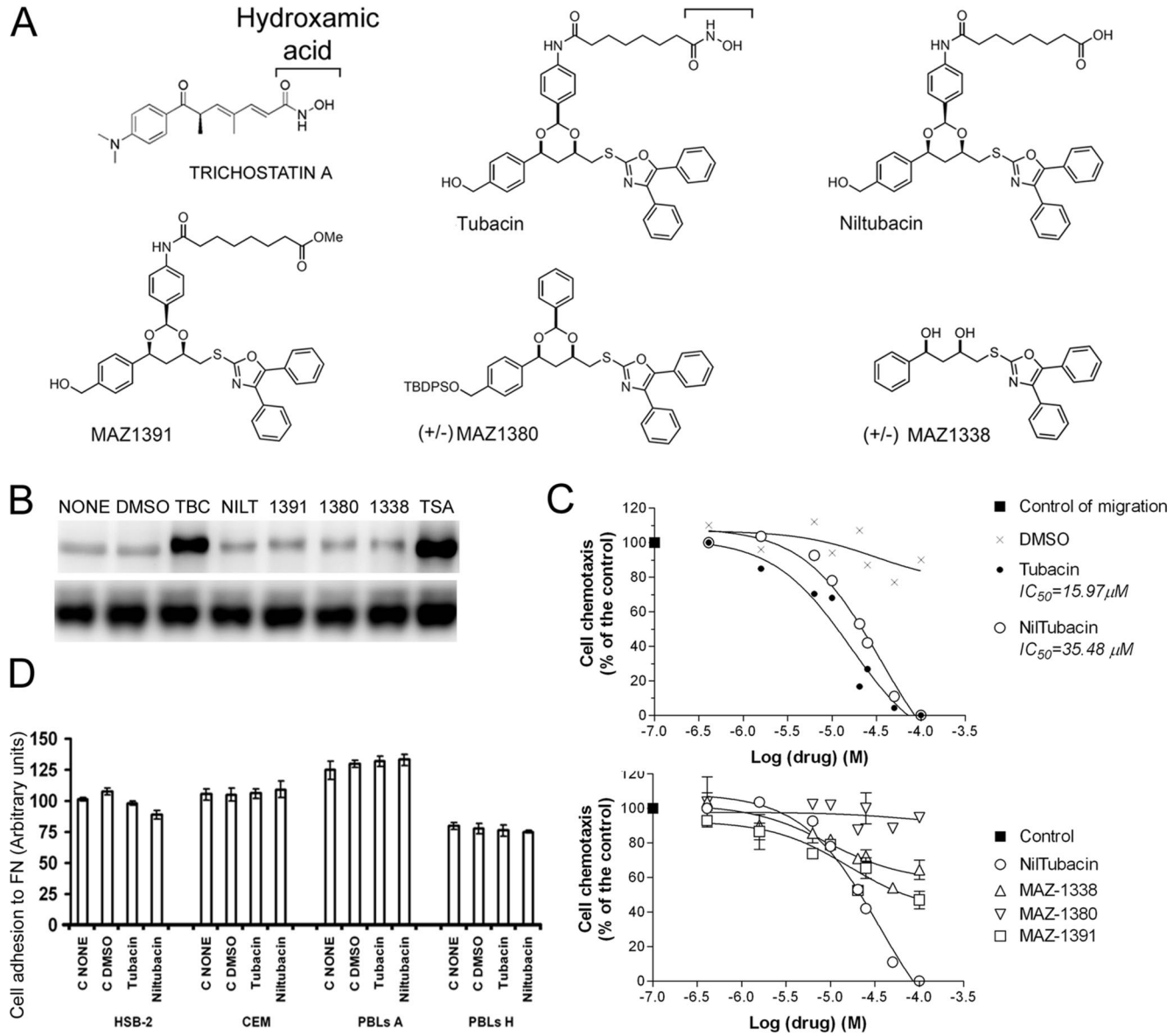

Figure 4. Effects of specific HDAC6 inhibitor tubacin and derivatives on lymphocyte chemotaxis. (A) Molecular structure of Tubacin and derivatives, where the Zn^{2+} chelating group is marked. TSA formula is also included. (B) Western-blot showing the tubulin acetylation levels in cells untreated or treated with 50 μM of the indicated chemical inhibitors is shown. (C) Cell migration assays in Transwell chambers. Dose-dependent inhibitory effects of HDAC6 targeting drugs on the chemotactic response of CEM T-cells to SDF-1α. (D) Adhesion to FN (20 μg/ml for T-cell lines and 50 μg/ml for PBLs) of lymphocytes untreated or treated with Tubacin and niltubacin. Four representative experiments are shown. Arbitrary units.

of PBLs, HSB-2, and CEM T-cells induced by SDF-1α (Figure 4C and unpublished data). Unexpectedly, the inactive compounds niltubacin, MAZ-1338, and MAZ-1391 also decreased cell migration (Figure 4C). In contrast, the inactive derivative MAZ-TBDPS-O-1380 did not exert this effect (Figure 4C). Neither tubacin nor niltubacin affected the adhesion of PBLs or T-cells to FN-80 in static conditions (Figure 4D). Likewise, no significant changes on cell viability and the expression levels of different adhesion and chemokine receptors were detected when CEM cells were treated with tubacin or niltubacin (Table 1B and unpublished data).

To further ascertain whether niltubacin was exerting its effects by binding to the same and/or overlapping site(s) as tubacin on the HDAC6 molecule, cross-competitive tubulin deacetylase functional assays were performed. Niltubacin prevented the inhibitory effect of tubulin deacetylase caused by tubacin, in a dose-dependent manner (Figure 5, A–C), thus indicating both molecules were interacting with the same and/or overlapping site(s) of the HDAC6 molecule. In parallel, migration assays showed that the combination of tubacin (0.5 μM) with increasing doses of niltubacin, which revert the tubacin-deacetylase inhibitory effect, resulted in a similar inhibition level of lymphocyte migration compared with same doses of tubacin alone (Figure 5D). Therefore, although tubacin is an active specific inhibitor of HDAC6 tubulin deacetylase, its effect on lymphocyte migration seems to be exerted independently of its inhibitory effect upon deacetylase enzymatic activity. Moreover, in

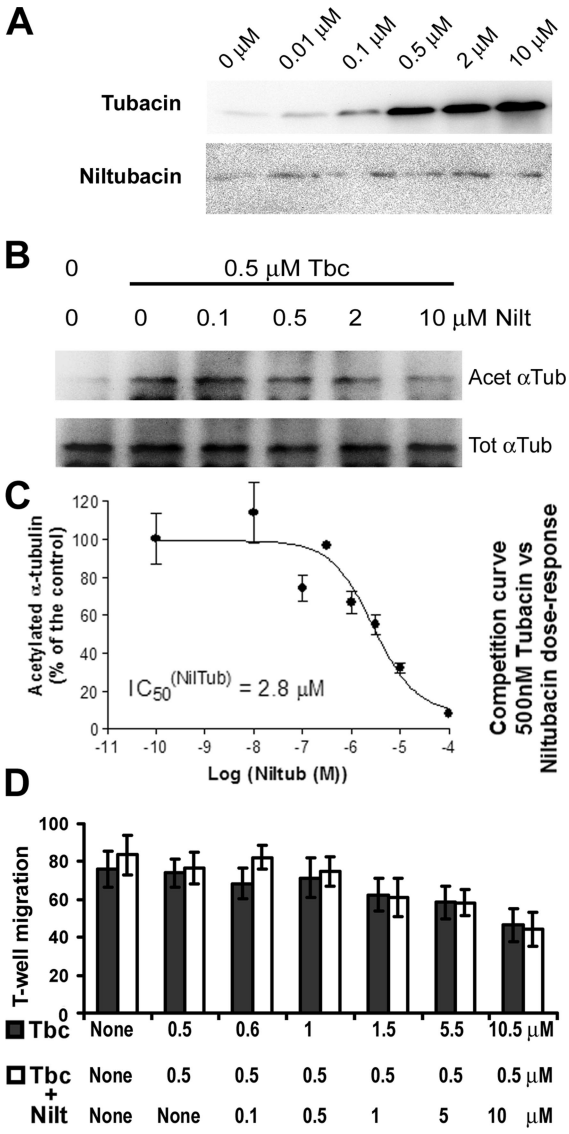

Figure 5. Niltubacin competes tubacin-mediated effect on HDAC6 tubulin deacetylase activity. (A) Effect on tubulin acetylation of increasing doses of tubacin or niltubacin. (B and C) Prevention of the tubacin inhibitory effect on HDAC6 tubulin deacetylase activity by niltubacin. Western blotting of a representative experiment (B) and competition curve of increasing doses of niltubacin versus 0.5 μM tubacin. Mean ± SD of four independent experiments is represented (C). (D) Inhibition of SDF-1α–directed migration by increasing doses of tubacin alone or 0.5 μM tubacin plus increasing doses of niltubacin. In each paired histograms, the same final amounts of tubacin alone (■) or Tubacin plus niltubacin (□) are represented.

T-lymphocyte polarization induced by the chemokine SDF-1α, similar results were observed in cells treated with TSA, tubacin or niltubacin, which suggest that HDAC6 tubulin deacetylase activity is neither essential for lymphocyte polarization (Figures 2 and 6) nor migration (Figures 4C and 5).

Overexpression of HDAC6 and the Deacetylase Dead Mutant Enhances T-Lymphocyte Migration

The effect of HDAC6 on lymphocyte migration was also analyzed. CEM T-cells were transduced and PBLs were

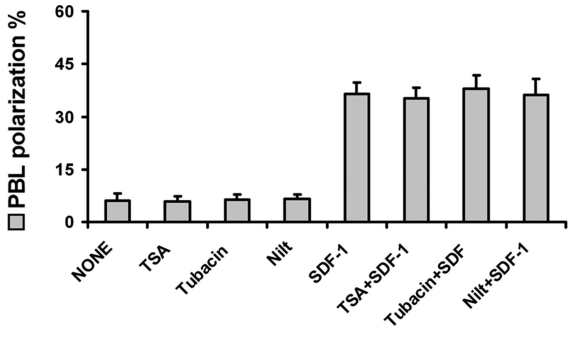

Figure 6. TSA, tubacin, and niltubacin do not modify the polarization of PBL induced by SDF-1. PBL were treated as indicated and then allowed to adhere to FN-coated coverslips for 15 min. Cells were then fixed and stained with an anti-ICAM-3 mAb followed by an FITC-labeled secondary antibody. Cell polarization was determined as stated in *Materials and Methods.* The arithmetic mean ± SD of three independent experiments is shown.

nucleofected to overexpress wtHDAC6-GFP or HDAC6 H216A/H611A-GFP (Figure 7, A and B, and 8A, respectively). We found that overexpression of wtHDAC6 or deacetylase dead mutant in CEM leukemic T-cells (Figure 7B) and PBLs (Figure 8A) exhibited enhanced transmigration when compared with GFP-alone overexpressing cells. Interestingly, migratory CEM cells overexpressing either HDAC6-GFP or HDAC6 H216A/H611A-GFP showed an accumulation of this enzyme at the cell leading edge and, in lesser extent, in the uropod (Figure 7C, Supplementary Videos 2 and 3, and unpublished data). In addition, the overexpression of HDAC6-GFP favored the adhesion and transmigration of CEM cells under flow conditions, whereas the rolling and detachment steps were proportionally significantly diminished (Figure 7D). Furthermore, the number of leukocyte–endothelium interactions was dramatically increased in the HDAC6-GFP–transduced cells (absolute values: 574 for pLZR-HDAC6 vs. 258 for pLZR-GFP or 327 for untransduced parental cells). These data concur with those obtained using the chemical HDAC6 inhibitor (Figure 3E). In conclusion, overexpression of both HDAC6 and the deacetylase dead mutant, which localizes at motility-related structures, enhances lymphocyte migration. Therefore, deacetylase activity appears to be dispensable for HDAC6-regulated chemotaxis.

Knocking Down of HDAC6 Inhibits Lymphocyte Chemotaxis

The effect of HDAC6 on lymphocyte chemotaxis was also analyzed by knocking down expression. We found that siRNA-HDAC6-interfered PBL and CEM cells showed a diminished expression of HDAC6 and a defective migratory activity in response to the chemokine SDF-1α (Figure 8, B–D). To unequivocally demonstrate that HDAC6 molecule itself was accounting for the above-described functional effects, HDAC6wt, and catalytically inactive HDAC6DD were compared in restoring the migration of HDAC6-interfered cells. The results convincingly show that defective cell migration is reverted at comparable level by overexpression of both HDAC6wt and HDAC6DD molecules (Figure 8C) and that the effect is HDAC6 specific. Moreover, adhesion and transmigration of HDAC6 knockdown CEM cells to activated HUVEC was assessed under shear stress conditions. As observed above for TSA-treated lymphocytes (Figure 3, E and F), a reduced number of adherent and transmigrated

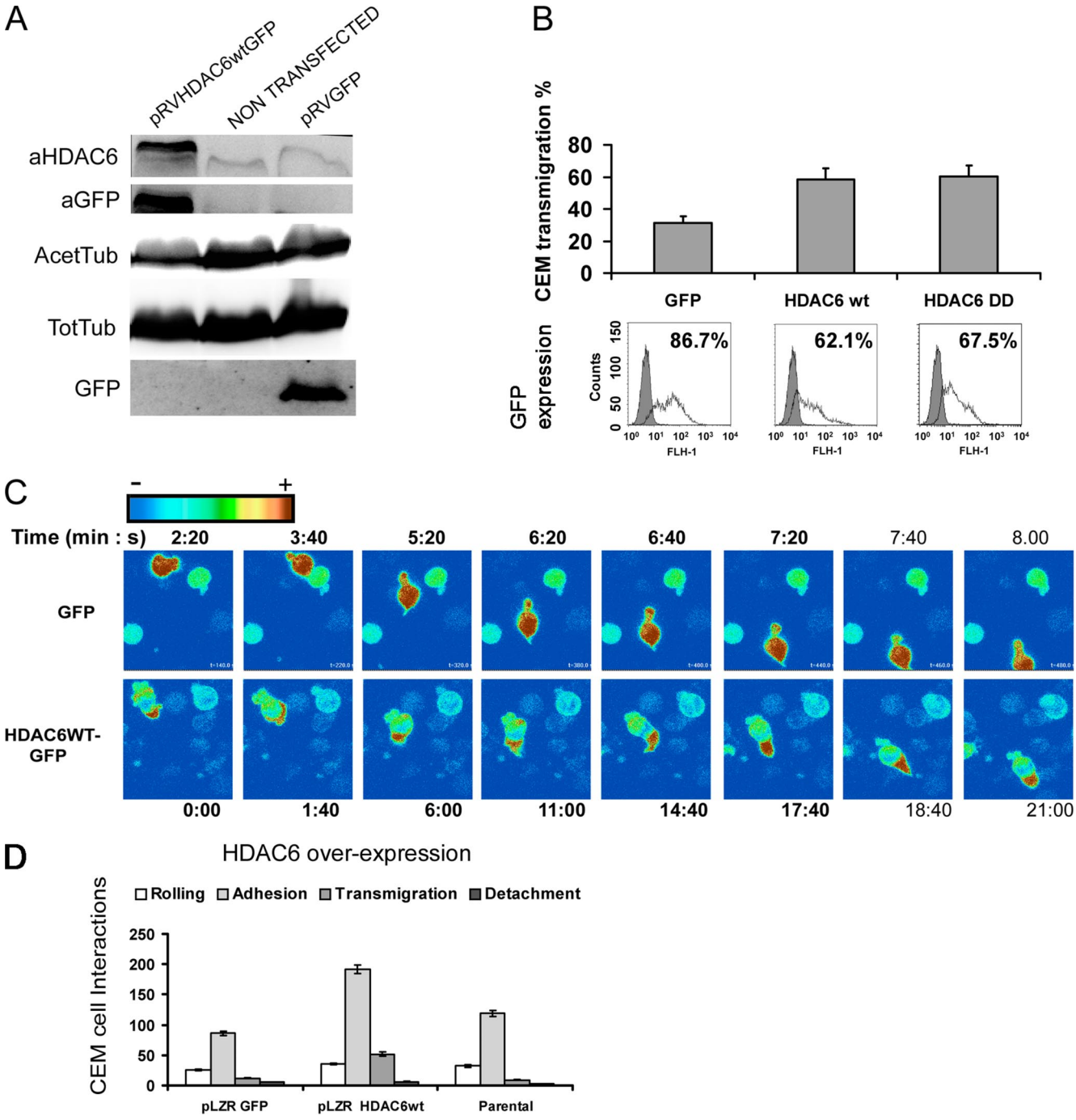

Figure 7. Functional effects of HDAC6 overexpression in T-cell migration. (A) CEM cells (1.0×10^7) transduced or not with GFP or HDAC6-GFP were lysed, sonicated, and immunoblotted with antibodies against the indicated molecules. (B) HDAC6-GFP overexpression enhanced the migratory behavior of CEM cells. Transduced CEM cells, overexpressing GFP alone, wtHDAC6-GFP or HDAC6 H216A/H611A-EGFP (HDAC6 DD) were allowed to transmigrate in Transwell chambers toward 100 ng/ml SDF-1. Fold induction ± SD of migrated cells of three different experiments is shown. Quantitative flow cytometric analyses of the expression levels by CEM cells transduced with GFP, HDAC6-GFP, and HDAC6DD-GFP. (C) Confocal videomicroscopy sequence showing the cellular distribution of GFP, or HDAC6-GFP in CEM cells. Image represents the fluorescence intensity of GFP in an arbitrary pseudocolor map (bar on top left). (D) HDAC6 enhances lymphocyte transendothelial migration under flow. Rolling, adhesion, transmigration, and detachment of HDAC6-overexpressing CEM cells under shear stress. Transendothelial migration of parental and transduced CEM cells (GFP alone or HDAC6-GFP) under shear stress across a TNF-α–activated HUVEC monolayer. The number of rolling (white bars), adhered (light gray tone bars), transmigrated (dark gray bars) and detached (black bars) cells were obtained as described in *Materials and Methods.* Data represent values ± SD from two independent experiments.

lymphocytes was found in HDAC6-knockdown cells (Figure 8D). These data show that the overexpression of HDAC6 enhances lymphocyte migration, whereas its targeting inhibits lymphocyte chemotaxis.

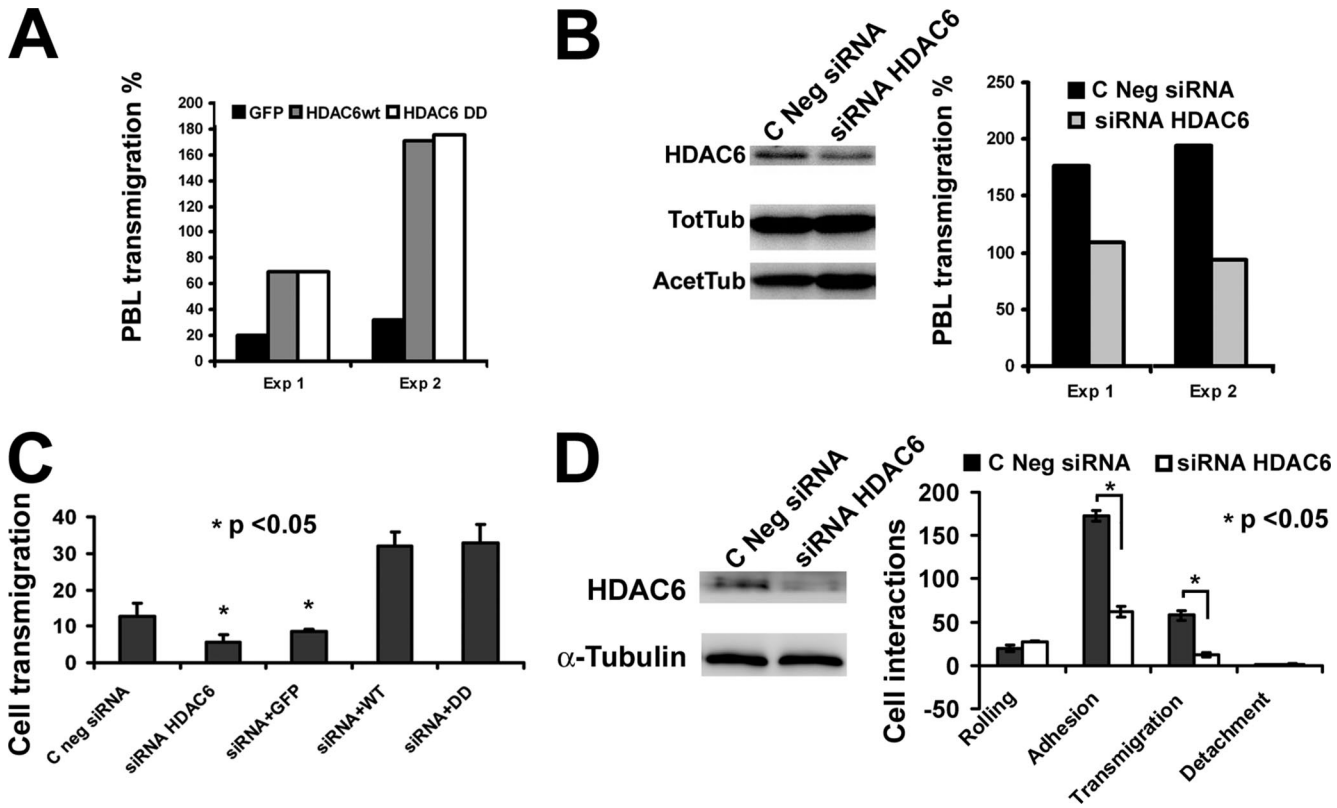

Figure 8. Regulation of the chemotactic and transmigration responses of lymphocytes by silencing of HDAC6. (A) HDAC6-GFP or HDAC6 H216A/H611A-GFP overexpression enhanced the migratory ability of PBLs versus GFP overexpression. Nucleofected PBLs overexpressing HDAC6-GFP, HDAC6 H216A/H611A (HDAC6 DD), or GFP were allowed to migrate toward a chemotactic gradient of 100 ng/ml SDF-1α in Transwell chambers. Two independent experiments with different healthy donors are shown. (B) Effect of HDAC6 knocking-down in PBL chemotaxis. Western blotting analysis of HDAC6 and acetylated tubulin in siRNA HDAC6-interfered PBLs. Two independent migration assays in Transwell chambers, with HDAC6 knocked-down PBLs versus mock nucleofected with control negative oligonucleotides from different healthy donors, are shown. (C) Rescue of defective migratory activity of HDAC6 knockdown cells. CEM cells were interfered with siRNA HDAC6, and 48 h later were transfected with either wild type or DD (double deacetylase dead mutant) and then assayed for chemotactic migration in Transwell chambers. (D) HDAC6 knockdown inhibits lymphocyte transendothelial migration under flow. Rolling, adhesion, transmigration, and detachment events were quantified for negative control siRNA (dark gray bars) and HDAC6 siRNA (white bars) treated cells under physiological shear stress on a TNF-α–activated HUVEC monolayer. The number of cells in each step was quantified as described in *Material and Methods*. Control Western blotting analysis of HDAC6 and alpha-tubulin in siRNA HDAC6-interfered CEM cells is shown. Data show mean values ± SD from four independent experiments.

DISCUSSION

Although the roles of tubulin cytoskeleton and microtubule acetylation in the migration of adherent cells have been studied (Joseph *et al.*, 1989; Terzis *et al.*, 1997; Westerlund *et al.*, 1997; Hubbert *et al.*, 2002; Haggarty *et al.*, 2003), little is known regarding its involvement in the motility of leukocytes. In this work, we have addressed the possible role of HDAC6 tubulin deacetylase in the migratory activity of T-lymphocytes. We have found that activated T-cells show increased levels of acetylated microtubules around the MTOC, partially colocalizing with HDAC6. It has been reported that the microtubular network is retracted toward the uropod in T-cells polarized by chemokines (Ratner *et al.*, 1997). On the other hand, we and others have previously shown that microtubules do not play an important role in uropod formation (Wilkinson, 1986; Campanero *et al.*, 1994; Brown *et al.*, 2001). Whether the enhanced levels of acetylated microtubules seen in polarized migrating T-lymphocytes are part of the mechanism by which microtubular bundles are retracted into the uropod or occur after retraction of the microtubule meshwork into this structure is still an open question. However, our data using different chemical inhibitors of HDAC6 and experiments with cells overexpressing HDAC6 deacetylase dead mutant do not support a role for tubulin deacetylase activity in the acquisition of a polarized migratory cell shape.

Our data on the localization of HDAC6 at motile protrusive structures, such as the leading edge and the uropod, support a possible involvement of this molecule in the regulation of lymphocyte locomotion. Accordingly, we found that the migration of T-cells in response to chemokines is reduced by HDAC6 siRNA and increased by HDAC6 overexpression and that these effects are not due to changes in cell adhesiveness under static conditions. Nevertheless, our data under shear stress conditions clearly indicate that adhesion strength is weaker in lymphocytes in which HDAC6 has been targeted by either a chemical inhibitor or specific siRNA knockdown. Hence, HDAC6 molecules appear to be required for adhesion and transmigration of lymphocytes under mechanical stress conditions or when cells transmigrate across constricted spaces. These data, together with similar results in mouse NIH3T3 fibroblasts (Hubbert *et al.*, 2002), suggest that HDAC6 levels modify molecular interactions or intracellular signaling pathways involved in the

modulation of cell motility. Interestingly, we have found that the levels of HDAC6 but not its deacetylase activity seems to be critical for lymphocyte chemotaxis. Hence, our data with a panel of tubacin derivatives, together with the results with cells overexpressing wt and deacetylase inactive forms of HDAC6, underscore the critical role of this molecule in lymphocyte motility regardless of its enzymatic activity. This is apparently in disagreement with data obtained in NIH3T3 fibroblasts, in which HDAC6 deacetylase activity was related to cell motility (Hubbert *et al.*, 2002; Haggarty *et al.*, 2003; Palazzo *et al.*, 2003). However, it is feasible that HDAC6 has a scaffold role for the rapid formation of molecular complexes required for lymphocyte migration, a process 10- to 20-fold faster than that of fibroblasts (Serrador *et al.*, 1999). Hence, very dynamic processes such as leukocyte locomotion would require a rapid HDAC6-mediated on/off assembly of molecular complexes, whereas this effect of HDAC6 would be dispensable in slow dynamic processes such as fibroblast locomotion or other phenomena involving cell-to-cell immune or viral-mediated interactions (Serrador *et al.*, 2004; Valenzuela-Fernandez *et al.*, 2005).

Little is known about the signal transduction pathways controlling HDAC6 activity. It has been recently described that HDAC6 forms complexes with phosphatases, including the catalytic subunit of PP1, and that HDAC6-PP1 interaction is disrupted by TSA (Brush *et al.*, 2004; Chen *et al.*, 2005). In addition, we have previously reported that tubulin acetylation diminishes in lymphocytes when the activity of RhoA is abolished (Vicente-Manzanares *et al.*, 2002). Furthermore, it is known that Rho GTPases coordinate the two poles of migrating T-lymphocytes (Sanchez-Madrid and del Pozo, 1999; Worthylake and Burridge, 2001) and control the dynamics of actin and tubulin cytoskeleton (Wittmann and Waterman-Storer, 2001; Ridley *et al.*, 2003). It is therefore feasible that HDAC6 has a role in the cross-talk between tubulin- and actin-associated molecules. This role of HDAC6 might explain the relationship between chemokines, Rho/mDia activation/inactivation (Vicente-Manzanares *et al.*, 2002; Palazzo *et al.*, 2004; Destaing *et al.*, 2005) and the consequences of targeting HDAC6 on cell migration (Hubbert *et al.*, 2002; Haggarty *et al.*, 2003; and this report). Whether Rho GTPases could regulate the activity of HDAC6 and its interaction with motor proteins is an interesting point to be explored. We propose that mechanisms such as alteration in signaling or relative PP1, HSP90, mDia, dynein, or tubulin dissociation from molecular complexes with HDAC6 (Kawaguchi *et al.*, 2003; Brush *et al.*, 2004; Bali *et al.*, 2005; Destaing *et al.*, 2005; Hideshima *et al.*, 2005; Kovacs *et al.*, 2005) could modulate lymphocyte migration independently of its deacetylase activity.

ACKNOWLEDGMENTS

We thank to Dr. Roberto González-Amaro for helpful correction and suggestions to this manuscript. We thank the National Cancer Institute and the Initiative for Chemical Genetics, who provided support for this publication. This work was supported by Grant BFU 2005–08435/BMC from the Spanish Ministry of Education and Science, the Ayuda a la Investigación Básica 2002 from Juan March Foundation and a grant from Lilly Foundation. J.M.S. is supported by Contrato-Investigador FIS from Instituto de Salud Carlos III.

REFERENCES

Alon, R., and Feigelson, S. (2002). From rolling to arrest on blood vessels: leukocyte tap dancing on endothelial integrin ligands and chemokines at sub-second contacts. Semin. Immunol. *14*, 93–104.

Bali, P. *et al.* (2005). Inhibition of histone deacetylase 6 acetylates and disrupts the chaperone function of heat shock protein 90, a novel basis for antileukemia activity of histone deacetylase inhibitors. J. Biol. Chem. *280*, 26729–26734.

Barreiro, O., Yanez-Mo, M., Sala-Valdes, M., Gutierrez-Lopez, M. D., Ovalle, S., Higginbottom, A., Monk, P. N., Cabanas, C., and Sanchez-Madrid, F. (2005). Endothelial tetraspanin microdomains regulate leukocyte firm adhesion during extravasation. Blood *105*, 2852–2861.

Barreiro, O., Yanez-Mo, M., Serrador, J. M., Montoya, M. C., Vicente-Manzanares, M., Tejedor, R., Furthmayr, H., and Sanchez-Madrid, F. (2002). Dynamic interaction of VCAM-1 and ICAM-1 with moesin and ezrin in a novel endothelial docking structure for adherent leukocytes. J. Cell Biol. *157*, 1233–1245.

Bertos, N. R., Gilquin, B., Chan, G. K., Yen, T. J., Khochbin, S., and Yang, X. J. (2004). Role of the tetradecapeptide repeat domain of human histone deacetylase 6 in cytoplasmic retention. J. Biol. Chem. *279*, 48246–48254.

Brown, M. J., Hallam, J. A., Colucci-Guyon, E., and Shaw, S. (2001). Rigidity of circulating lymphocytes is primarily conferred by vimentin intermediate filaments. J. Immunol. *166*, 6640–6646.

Brush, M. H., Guardiola, A., Connor, J. H., Yao, T. P., and Shenolikar, S. (2004). Deactylase inhibitors disrupt cellular complexes containing protein phosphatases and deacetylases. J. Biol. Chem. *279*, 7685–7691.

Campanero, M. R., Sánchez-Mateos, P., del Pozo, M. A., and Sánchez-Madrid, F. (1994). ICAM-3 regulates lymphocyte morphology and integrin-mediated T cell interaction with endothelial cell and extracellular matrix ligands. J. Cell Biol. *127*, 867–878.

Chen, C. S., Weng, S. C., Tseng, P. H., and Lin, H. P. (2005). Histone acetylation-independent effect of histone deacetylase inhibitors on Akt through the reshuffling of protein phosphatase 1 complexes. J. Biol. Chem. *280*, 38879–38887.

del Pozo, M. A., Sanchez-Mateos, P., Nieto, M., and Sanchez-Madrid, F. (1995). Chemokines regulate cellular polarization and adhesion receptor redistribution during lymphocyte interaction with endothelium and extracellular matrix. Involvement of cAMP signaling pathway. J. Cell Biol. *131*, 495–508.

Destaing, O., Saltel, F., Gilquin, B., Chabadel, A., Khochbin, S., Ory, S., and Jurdic, P. (2005). A novel Rho-mDia2-HDAC6 pathway controls podosome patterning through microtubule acetylation in osteoclasts. J. Cell Sci. *118*, 2901–2911.

Etienne-Manneville, S., and Hall, A. (2002). Rho GTPases in cell biology. Nature *420*, 629–635.

Furumai, R., Komatsu, Y., Nishino, N., Khochbin, S., Yoshida, M., and Horinouchi, S. (2001). Potent histone deacetylase inhibitors built from trichostatin A and cyclic tetrapeptide antibiotics including trapoxin. Proc. Natl. Acad. Sci. USA *98*, 87–92.

Gundersen, G. G., Kreitzer, G., Cook, T., and Liao, G. (1998). Microtubules as determinants of cellular polarity. Biol. Bull. *194*, 358–360.

Haggarty, S. J., Koeller, K. M., Wong, J. C., Grozinger, C. M., and Schreiber, S. L. (2003). Domain-selective small-molecule inhibitor of histone deacetylase 6 (HDAC6)-mediated tubulin deacetylation. Proc. Natl. Acad. Sci. USA *100*, 4389–4394.

Hideshima, T., Bradner, J. E., Wong, J., Chauhan, D., Richardson, P., Schreiber, S. L., and Anderson, K. C. (2005). Small-molecule inhibition of proteasome and aggresome function induces synergistic antitumor activity in multiple myeloma. Proc. Natl. Acad. Sci. USA *102*, 8567–8572.

Hubbert, C., Guardiola, A., Shao, R., Kawaguchi, Y., Ito, A., Nixon, A., Yoshida, M., Wang, X. F., and Yao, T. P. (2002). HDAC6 is a microtubule-associated deacetylase. Nature *417*, 455–458.

Jose, B., Okamura, S., Kato, T., Nishino, N., Sumida, Y., and Yoshida, M. (2004). Toward an HDAC6 inhibitor: synthesis and conformational analysis of cyclic hexapeptide hydroxamic acid designed from alpha-tubulin sequence. Bioorg. Med. Chem. *12*, 1351–1356.

Joseph, J. P., Grierson, I., and Hitchings, R. A. (1989). Taxol, cytochalasin B and colchicine effects on fibroblast migration and contraction: a role in glaucoma filtration surgery? Curr. Eye Res. *8*, 203–215.

Kawaguchi, Y., Kovacs, J. J., McLaurin, A., Vance, J. M., Ito, A., and Yao, T. P. (2003). The deacetylase HDAC6 regulates aggresome formation and cell viability in response to misfolded protein stress. Cell *115*, 727–738.

Kouzarides, T. (2000). Acetylation: a regulatory modification to rival phosphorylation? EMBO J. *19*, 1176–1179.

Kovacs, J. J., Murphy, P. J., Gaillard, S., Zhao, X., Wu, J. T., Nicchitta, C. V., Yoshida, M., Toft, D. O., Pratt, W. B., and Yao, T. P. (2005). HDAC6 regulates Hsp90 acetylation and chaperone-dependent activation of glucocorticoid receptor. Mol. Cell. *18*, 601–607.

L'Hernault, S. W., and Rosenbaum, J. L. (1983). Chlamydomonas alpha-tubulin is posttranslationally modified in the flagella during flagellar assembly. J. Cell Biol. *97*, 258–263.

Mackay, C. R. (2001). Chemokines: immunology's high impact factors. Nat. Immunol. *2*, 95–101.

Matsuyama, A. *et al.* (2002). In vivo destabilization of dynamic microtubules by HDAC6-mediated deacetylation. EMBO J. *21*, 6820–6831.

Moreno, R. D., and Schatten, G. (2000). Microtubule configurations and post-translational alpha-tubulin modifications during mammalian spermatogenesis. Cell Motil. Cytoskelet. *46*, 235–246.

Palazzo, A., Ackerman, B., and Gundersen, G. G. (2003). Cell biology: tubulin acetylation and cell motility. Nature *421*, 230.

Palazzo, A. F., Eng, C. H., Schlaepfer, D. D., Marcantonio, E. E., and Gundersen, G. G. (2004). Localized stabilization of microtubules by integrin- and FAK-facilitated Rho signaling. Science *303*, 836–839.

Pantaloni, D., Le Clainche, C., and Carlier, M. F. (2001). Mechanism of actin-based motility. Science *292*, 1502–1506.

Piperno, G., and Fuller, M. T. (1985). Monoclonal antibodies specific for an acetylated form of alpha-tubulin recognize the antigen in cilia and flagella from a variety of organisms. J. Cell Biol. *101*, 2085–2094.

Piperno, G., LeDizet, M., and Chang, X. J. (1987). Microtubules containing acetylated alpha-tubulin in mammalian cells in culture. J. Cell Biol. *104*, 289–302.

Polevoda, B., and Sherman, F. (2002). The diversity of acetylated proteins. Genome Biol. *3*, reviews 0006.

Pollard, T. D., and Borisy, G. G. (2003). Cellular motility driven by assembly and disassembly of actin filaments. Cell *112*, 453–465.

Prescott, A. R., Vestberg, M., and Warn, R. M. (1989). Microtubules rich in modified alpha-tubulin characterize the tail processes of motile fibroblasts. J. Cell Sci. *94*, 227–236.

Ratner, S., Sherrod, W. S., and Lichlyter, D. (1997). Microtubule retraction into the uropod and its role in T cell polarization and motility. J. Immunol. *159*, 1063–1067.

Ridley, A. J., Schwartz, M. A., Burridge, K., Firtel, R. A., Ginsberg, M. H., Borisy, G., Parsons, J. T., and Horwitz, A. R. (2003). Cell migration: integrating signals from front to back. Science *302*, 1704–1709.

Sanchez-Madrid, F., and del Pozo, M. A. (1999). Leukocyte polarization in cell migration and immune interactions. EMBO J. *18*, 501–511.

Schulze, E., and Kirschner, M. (1987). Dynamic and stable populations of microtubules in cells. J. Cell Biol. *104*, 277–288.

Serrador, J. M., Alonso-Lebrero, J. L., del Pozo, M. A., Furthmayr, H., Schwartz-Albiez, R., Calvo, J., Lozano, F., and Sanchez-Madrid, F. (1997). Moesin interacts with the cytoplasmic region of intercellular adhesion molecule-3 and is redistributed to the uropod of T lymphocytes during cell polarization. J. Cell Biol. *138*, 1409–1423.

Serrador, J. M., Cabrero, J. R., Sancho, D., Mittelbrunn, M., Urzainqui, A., and Sanchez-Madrid, F. (2004). HDAC6 deacetylase activity links the tubulin cytoskeleton with immune synapse organization. Immunity *20*, 417–428.

Serrador, J. M., Nieto, M., and Sanchez-Madrid, F. (1999). Cytoskeletal rearrangement during migration and activation of T lymphocytes. Trends Cell Biol. *9*, 228–233.

Small, J. V., and Kaverina, I. (2003). Microtubules meet substrate adhesions to arrange cell polarity. Curr. Opin. Cell Biol. *15*, 40–47.

Tannenbaum, J., and Slepecky, N. B. (1997). Localization of microtubules containing posttranslationally modified tubulin in cochlear epithelial cells during development. Cell Motil. Cytoskelet. *38*, 146–162.

Terzis, A. J., Thorsen, F., Heese, O., Visted, T., Bjerkvig, R., Dahl, O., Arnold, H., and Gundersen, G. (1997). Proliferation, migration and invasion of human glioma cells exposed to paclitaxel (Taxol) in vitro. Br. J. Cancer *75*, 1744–1752.

Valenzuela-Fernandez, A. *et al.* (2005). Histone deacetylase 6 regulates human immunodeficiency virus type 1 infection. Mol. Biol. Cell *16*, 5445–5454.

Verdel, A., Curtet, S., Brocard, M. P., Rousseaux, S., Lemercier, C., Yoshida, M., and Khochbin, S. (2000). Active maintenance of mHDA2/mHDAC6 histone-deacetylase in the cytoplasm. Curr. Biol. *10*, 747–749.

Vicente-Manzanares, M., Cabrero, J. R., Rey, M., Perez-Martinez, M., Ursa, A., Itoh, K., and Sanchez-Madrid, F. (2002). A role for the Rho-p160 Rho coiled-coil kinase axis in the chemokine SDF-1 alpha-induced lymphocyte actomyosin and microtubular organization and chemotaxis. J. Immunol. *168*, 400–410.

Vicente-Manzanares, M., and Sanchez-Madrid, F. (2004). Role of the cytoskeleton during leukocyte responses. Nat. Rev. Immunol. *4*, 110–122.

von Andrian, U. H., and Mackay, C. R. (2000). T-cell function and migration. Two sides of the same coin. N. Engl. J. Med. *343*, 1020–1034.

Westerlund, A., Hujanen, E., Hoyhtya, M., Puistola, U., and Turpeenniemi-Hujanen, T. (1997). Ovarian cancer cell invasion is inhibited by paclitaxel. Clin. Exp. Metast. *15*, 318–328.

Wilkinson, P. C. (1986). The locomotor capacity of human lymphocytes and its enhancement by cell growth. Immunology *57*, 281–289.

Wittmann, T., and Waterman-Storer, C. M. (2001). Cell motility: can Rho GTPases and microtubules point the way? J. Cell Sci. *114*, 3795–3803.

Worthylake, R. A., and Burridge, K. (2001). Leukocyte transendothelial migration: orchestrating the underlying molecular machinery. Curr. Opin. Cell Biol. *13*, 569–577.

Zhang, Y., Li, N., Caron, C., Matthias, G., Hess, D., Khochbin, S., and Matthias, P. (2003). HDAC-6 interacts with and deacetylates tubulin and microtubules in vivo. EMBO J. *22*, 1168–1179.